

ESTIMATING THE EXTENT OF DAMAGE TO WASTE PACKAGE SURFACES BY LOCALIZED CORROSION IN POTENTIAL DISPOSAL ENVIRONMENTS

Pavan Shukla, Roberto Pabalan, and Osvaldo Pensado

*Center for Nuclear Waste Regulatory Analyses (CNWRA[®])
Southwest Research Institute[®]
San Antonio, Texas 78238
pshukla@cnwra.swri.edu*

In a performance assessment model, important parameters needed to compute the consequences of radionuclide release to the environment include the failure time of packages enclosing waste forms and the extent of damage to the waste package surface. Radionuclide releases from the waste package are a function of the extent of damage, generally specified in the form of a surface fraction, because the dimension of this damage or breach area constrains radionuclide release by advection and diffusion. This paper proposes methodologies for estimating the extent of damage to the waste package surface induced by localized corrosion in different potential disposal systems. The methodologies are developed considering physico-chemical processes such as availability and viability of cathodic reactions to sustain anodic reactions that cause localized corrosion of waste package materials. In particular, the methodologies account for factors such as (i) the type and rate of cathodic reactions available to sustain the anodic reactions, (ii) the rate of metal dissolution due to anodic reactions, and (iii) the electrochemical driving force necessary to initiate and propagate localized corrosion. The methodologies are applied to estimate the breach area for carbon- and stainless-steel waste package material in different potential disposal environments.

I. INTRODUCTION

Estimating the extent of damage to a waste package due to localized corrosion is challenging. Information on the extent of damage due to localized corrosion is needed in performance assessment models to estimate consequences of radionuclide release to the environment. Radionuclide release can only occur after engineered barriers, such as the waste package, are compromised. An expected degradation mode of metallic waste packages is corrosion. For a wide range of environmental conditions, chemical degradation takes the form of localized corrosion, under which waste packages could be compromised in a relatively short period. Detailed

performance assessments commonly evaluate radionuclide release consequences associated with localized corrosion as initiating events. In general, release consequences are a function of the time of waste package failure and the extent of damage to the waste package surface. Therefore, the extent of damage, expressed as a fraction of the waste package area, is an important parameter.

This paper proposes a model for estimating the extent of damage to the waste package surface by localized corrosion in different potential disposal environments. The model is developed considering physico-chemical processes such as availability and viability of cathodic reactions to sustain anodic reactions that cause localized corrosion of waste package materials. In particular, the model accounts for factors such as (i) the type and rate of cathodic reactions available to sustain the anodic reactions, (ii) the rate of metal dissolution due to anodic reactions, and (iii) the electrochemical driving force necessary to initiate and propagate localized corrosion. The model is applied to estimate the waste package open area, also referred to as breach area, for carbon- and stainless-steel, which have been proposed as waste package material in different disposal environments. This model is based on the anodic propagation of localized corrosion. More work is warranted in the future to relate damage to the waste package wall with an expected decrease in the total rate of the anodic reactions due to the accumulation of damage (e.g., after penetration through the wall). Other factors could exist affecting the extent of the damage such as surface conditions of cathodic area or ionic transport in the active area.

II. MODEL

A localized corrosion model is presented for estimating the breach area on carbon- and stainless-steel waste packages. A schematic diagram of the localized corrosion process in the form of crevice corrosion is presented in Fig. 1. As seen in the figure, the anodic and

cathodic reactions are physically separated in the crevice corrosion process. The metal dissolution (i.e., anodic reactions) predominantly takes place under the crevice former. In the region adjacent to the crevice, both anodic and cathodic reactions take place. However, the rate of anodic and cathodic reactions is dependent upon the electric potential distribution and the presence of oxy-hydroxide films. The rate of anodic reactions is generally much lower than the rate of cathodic reactions

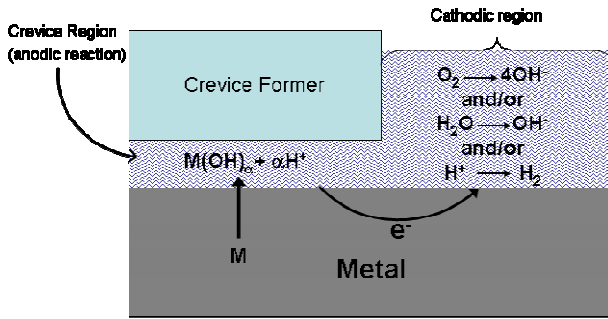


Fig. 1. Schematic diagram of the crevice corrosion process. The metal dissolution reactions take place in the crevice region, and the reduction reactions take place in the cathodic region.

immediately outside the crevice region, thus, an excess cathodic current is generated because the rate of cathodic reactions exceeds that of anodic reactions in the outside region. The excess cathodic current is necessary to sustain the anodic reactions underneath the crevice.¹

Under the free corrosion condition, the overall anodic current generated by the anodic reactions underneath the crevice must balance the excess cathodic current.² This statement can be represented by the following equation

$$I_A + I_C = 0 \quad (1)$$

where

- I_A — overall anodic current generated by the metal dissolution reactions underneath the crevice [A]
- I_C — excess cathodic current generated by the cathodic reactions in the outside region [A]

I_C is also referred to as cathodic capacity. The aforementioned also applies to the pitting corrosion. Under localized corrosion conditions, if the propagation rate, the rate of the cathodic reactions as a function of the electrode potential, and the electrode potential distribution outside the crevice is known, the maximum area of the waste package surface (i.e., the breach area) that could undergo localized corrosion can be estimated by invoking Eq. (1) and following the approach outlined in Ref. 2. However, the electrode potential distribution in the outer region is relatively uncertain and, thus, difficult to model.

The following approach is proposed to overcome the lack of information about the electrode potential distribution outside the crevice. It is widely accepted that localized corrosion in the form of crevice corrosion can initiate and be sustained when the corrosion potential, denoted by E_{corr} , is greater than the repassivation potential, denoted by E_{rp} .³⁻⁵ Similarly, pitting corrosion can initiate when E_{corr} is greater than the breakdown potential, denoted by E_{bd} .⁶ A schematic diagram depicting polarization of hypothetical anodic and cathodic reactions as a function of the electrode potential is presented in Fig. 2. According to the polarizations of the anodic and cathodic reactions in Fig. 2, the electrode is susceptible to crevice corrosion because E_{corr} is greater than E_{rp} . The electrode potential inside a crevice on the electrode is expected to be more cathodic than E_{rp} , and the electrode potential in the outer region is expected to be more anodic than E_{rp} . Because the electrode potential distribution is not known in the outer region, it can be assumed that the cathodic reactions are occurring at E_{rp} . This assumption will give a conservative estimate of breach area because the estimated excess cathodic current will be higher than the actual value as a result of the potential distribution in the outer region.

Considering the aforementioned assumption in Eq. (1), the breach area for a waste package surface undergoing crevice corrosion can be estimated according to the following equation

$$\frac{x PR F \rho A}{W_e} = (1 - x) A i_{cat, rp} \quad (2)$$

where

- | | | |
|---------------|---|--|
| x | — | breach area fraction of the waste package surface undergoing localized corrosion |
| PR | — | localized corrosion penetration rate [m/sec] |
| F | — | Faraday constant (96,485 C/mol) |
| ρ | — | density of the waste package material [kg/m ³] |
| A | — | surface area of the waste package [m ²] |
| W_e | — | equivalent weight of the waste package material [kg/mol] |
| $i_{cat, rp}$ | — | current density of the cathodic reaction at E_{rp} [A/m ²] |

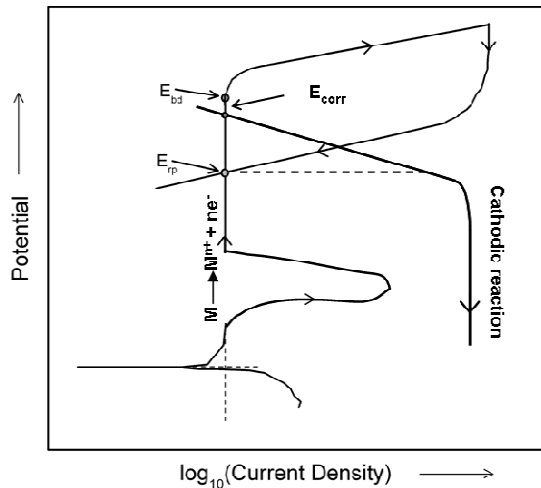


Fig. 2. Hypothetical anodic and cathodic reactions taking place as a function of electrode potential.

Eq. (2) can also be used to estimate the breach area of a waste package undergoing pitting corrosion by replacing $i_{cat, rp}$ with $i_{cat, bp}$, which denotes the current density of the cathodic reaction at E_{bp} . Application of Eq. (2) will provide the value of breach area fraction, x , which can be further used to estimate the breach area by multiplying x with the total area of the waste package surface. The model is applied to carbon- and stainless-steels in three different disposal environments, which are detailed next.

III. DISPOSAL ENVIRONMENTS

Many countries consider disposal of carbon- and stainless-steel waste packages in rock salt, clay, and granite.⁷ Different chemical and thermal conditions could arise around the waste packages when placed in these three representative disposal environments. These conditions are discussed next, as are the electrochemical conditions needed to estimate the breach area fraction.

III. A. Chemical and Thermal Conditions

Carbon- and stainless-steel waste packages placed in rock salts could be surrounded by sodium chloride or magnesium chloride brines of concentrations approximately equal to 26 and 30 wt %, respectively. The pH of the sodium-chloride-rich brines and magnesium-chloride-rich brines could range from 4–7. The temperature of the brines could range from 90–150 °C (194–302 °F). When the waste packages are placed inside bentonite clay, a solution predominantly containing sodium, magnesium, and chloride ions would surround the waste packages. The chemical composition of such a solution can be found in Table 2–15 of the European Commission report.⁷ Based on proposed designs, the maximum temperature of the solution could

range from 50–100 °C (122–212 °F). If the waste packages are placed in granite, an aqueous solution containing sodium chloride could develop in the disposal environment. The concentration of the sodium chloride would vary such that the chloride ion concentration could range from 50–50,000 parts per million (4.2×10^{-4} to 0.42 lb/gallon), and the solution temperature could be as high as 90 °C (194 °F).⁷ In this paper, it is assumed that the solution surrounding the waste packages in a granite rock disposal environment has a NaCl concentration of 50 g/L (0.42 lb/gallon) and the solution temperature is 90 °C (194 °F). In the three representative disposal environments, the chemical solutions surrounding the waste packages will initially have dissolved oxygen because the oxygen is expected to fill in the pores of the excavated disposal site.⁷ The solutions should eventually become anoxic as dissolved oxygen is consumed by oxygen reduction reactions.

III. B. Electrochemical Conditions

The electrochemical conditions for the carbon- and 316 stainless-steel waste package materials in the three disposal environments were calculated using the OLIAnalyzer Version 3.1 software.⁸ The software generated data for several systems have been extensively validated.⁹ The chemical compositions of the carbon- and 316 stainless-steel are provided in Table I. The chemical, thermal, and alloy specifications were input into the software. The calculated results included polarization curves and corrosion and repassivation potentials. The values of the cathodic current densities at the calculated repassivation potentials were read from the polarization curves.

TABLE I. Chemical Composition of the Carbon- and 316 Stainless-Steels

Alloy	Mass fraction of the various constituents					
	Fe	C	Mn	Mo	Cr	Ni
Carbon steel	0.967	0.023	9.98e-3	0	0	0
316 stainless steel	0.671	4.66e-3	0	0.018	0.183	0.124

Both chemical and calculated electrochemical conditions for the carbon steel in the three representative disposal environments are listed in Table II. Similarly, the chemical and electrochemical conditions for the 316 stainless steel are listed in Table I. The data in Tables II and III indicate that the cathodic current densities at the repassivation potentials of carbon- and 316 stainless-steels could range from 10^{-4} – $30 \mu\text{A}/\text{cm}^2$ (6.5×10^{-4} – $194 \mu\text{A}/\text{in}^2$).

IV. RESULTS AND DISCUSSION

The model is applied to calculate the breach area fraction as a function of cathodic current densities at the repassivation potentials and localized corrosion penetration rates. The model also needs the values of the densities and equivalent weights of the carbon- and 316 stainless-steel. The densities of the carbon- and stainless-steel are 7,860 and 7,890 kg/m³ (479.5 and 492.5 lb/ft³), respectively, and equivalent weights of the carbon- and

stainless-steel are 27.9 and 26 g/mol (0.061 and 0.057 lb/mol), respectively. Because there is only a marginal difference between densities and equivalent weights of the two alloys, the model is applied for carbon steel only. The calculated values of the breach area fraction as a function of the cathodic current densities and penetration rates are presented in Fig. 3. The calculated

TABLE II. Chemical and Electrochemical Conditions for Carbon Steel in the Three Representative Disposal Environments

Representative Disposal Environments	Chemical Conditions			Electrochemical Conditions			
	Chemical Compositions	pH Range	Temperature °C (°F)	Oxic Conditions		Anoxic Condition	
				E_{rp} (V vs. SHE [#])	$i_{cat, rp}$ $\mu\text{A}/\text{cm}^2$ ($\mu\text{A}/\text{in}^2$)	E_{rp} (V vs. SHE [#])	$i_{cat, rp}$ $\mu\text{A}/\text{cm}^2$ ($\mu\text{A}/\text{in}^2$)
Rock salt	26 wt % NaCl solution	4–7	90 (194)	-0.65	10 (64.5)	-0.65	10 (64.5)
	26 wt % NaCl solution	4–7	150 (302)	-0.76	9 (58.1)	-0.76	26 (167.7)
	30 wt % MgCl ₂ solution	4–5	90 (194)	-0.65	1 (6.5)	-0.65	12 (77.4)
	30 wt % MgCl ₂ solution	4–5	150 (302)	-0.78	10 (64.5)	-0.78	12 (77.4)
Bentonite clay	Bentonite clay water*		50 (122)	-0.52	20 (129.0)	-0.52	2 (12.9)
Granite	50 g/L (0.42 lb/gallon) NaCl solution	6–9	90 (194)	-0.6	22 (142.0)	-0.6	10 (64.5)

*The chemical composition of the bentonite clay water (i.e., solution around the waste packages in the bentonite clay) can be found in Table 2-15 of a European Commission report.⁷

[#]SHE stands for standard hydrogen electrode.

TABLE III. Chemical and Electrochemical Conditions for Stainless Steel in the Three Representative Disposal Environments

Representative Disposal Environment	Chemical Conditions			Electrochemical Conditions			
	Chemical Composition	pH Range	Temperature °C (°F)	Oxic Conditions		Anoxic Condition	
				E_{rp} (V vs. SHE [#])	$i_{cat, rp}$ $\mu\text{A}/\text{cm}^2$ ($\mu\text{A}/\text{in}^2$)	E_{rp} (V vs. SHE [#])	$i_{cat, rp}$ $\mu\text{A}/\text{cm}^2$ ($\mu\text{A}/\text{in}^2$)
Rock salt	26 wt % NaCl solution	4–7	90 (194)	-0.14	6 (38.7)	-0.14	1 [6.5]
	26 wt % NaCl solution	4–7	150 (302)	-0.25	8 (51.6)	-0.25	3 (193.5)
	30 wt % MgCl ₂ solution	4–5	90 (194)	-0.20	1 (6.5)	-0.20	0.07 (0.5)
	30 wt % MgCl ₂ solution	4–5	150 (302)	-0.32	1 (6.5)	-0.32	0.08 (0.5)
Bentonite clay	Bentonite clay water*		50 (122)	-0.08	20 (129.0)	-0.08	10^{-4} (6.5×10^{-4})
Granite	50 g/L (0.42 lb/gallon) NaCl solution	6–9	90 (194)	-0.05	13 (83.9)	-0.05	10^{-2} (6.5×10^{-2})

*The chemical composition of the bentonite clay water (i.e., solution around the waste packages in the bentonite clay) can be found in Table 2-15 of a European Commission report.⁷

[#]SHE stands for standard hydrogen electrode.

results do not account for the fact that the dissolved oxygen concentration in the solutions will change with time; therefore, the cathodic current densities will also change with time when solutions have dissolved oxygen. Moreover, it is also assumed that the chemical and thermal conditions do not change with time; hence, the cathodic current density is also constant. Because of the aforementioned assumptions, it is implied that the breach area fraction in a disposal environment is only a function of the cathodic current density, which is invariant with time.

As seen in Fig. 3, the breach area fraction increases with the cathodic current density. This result is consistent with the fact that more cathodic current is available to support several crevice sites at the waste package surface

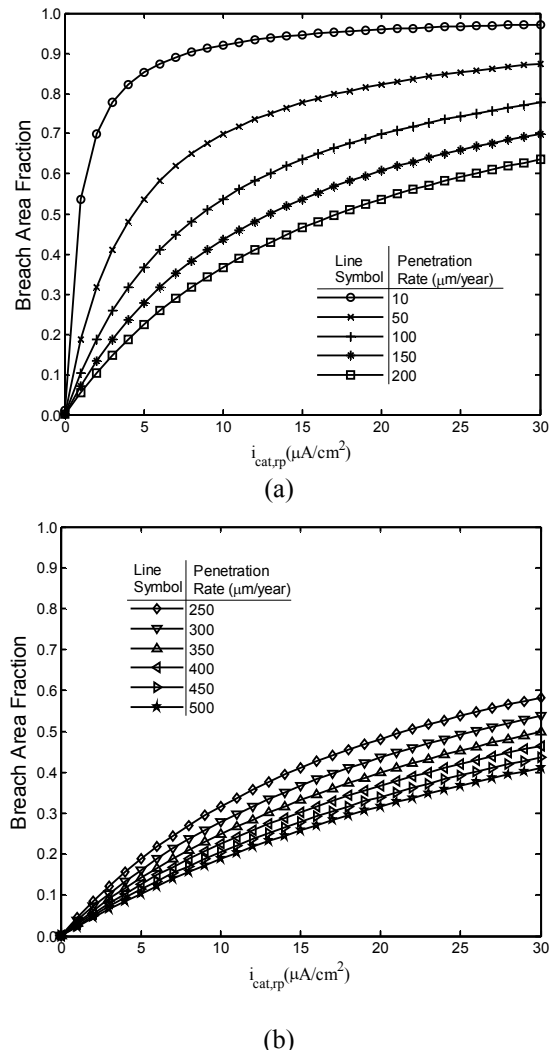


Fig. 3. Calculated breach area fraction as a function of cathodic current density at repassivation potential. The values of the localized corrosion penetration rates were varied. Penetration rates range from (a) 10–200 $\mu\text{m}/\text{year}$ (0.394–7.88 mils/year) and (b) 250–500 $\mu\text{m}/\text{year}$ (9.85–19.7 mils/year).

with increasing cathodic current density. It is also observed that the breach area fraction decreases with increasing penetration rate at a fixed value of the cathodic current density. This result is also consistent with the fact that the increasing penetration rate would require more and more cathodic current. Because the waste package area is fixed, only limited crevice sites could be supported by the excess cathodic current. Therefore, the breach area fraction decreases with increasing penetration rate at a fixed value of the cathodic current density. The calculated results are consistent with the physico-chemical model for crevice corrosion.

The model results should be used with caution especially for carbon-steel waste packages. The pitting factor, which is defined as ratio of the penetration depth by pitting to the penetration depth by general corrosion, for carbon-steel under oxidizing conditions varies between 1 to 3 (e.g., Johnson and King¹⁰). Therefore, the breach area will be close to unity when oxidizing conditions prevail and carbon-steel is susceptible to localized corrosion in a given disposal environment.

V. CONCLUSION

The proposed model provides consistent values of the breach area fraction as a function of the cathodic current density and penetration rates. The model can be used to estimate the breach area fraction of a waste package susceptible to localized corrosion in a disposal environment. The model can be used as long as relevant parameters such as penetration rate, repassivation potential, and cathodic current density at the repassivation potential are available. Even though the model applicability has been demonstrated for localized corrosion in form of crevice corrosion only, the model can be used also to estimate the breach area fraction for waste packages susceptible to the pitting corrosion.

ACKNOWLEDGMENTS

This paper describes work performed by the Center for Nuclear Waste Regulatory Analyses (CNWRA[®]) and its contractors for the U.S. Nuclear Regulatory Commission (USNRC) under Contract No. NRC-02-07-006. The activities reported here were performed on behalf of the USNRC Office of Nuclear Material Safety and Safeguards, Division of High-Level Waste Repository Safety.

This paper is an independent product of CNWRA and does not necessarily reflect the view or regulatory position of USNRC.

REFERENCES

1. R. G. KELLY, A. AGARWAL, F. CUI, X. SHAN, U. LANDAU, and J. PAYER, "Considerations of the Role of the Cathodic Regions in Localized Corrosion," *11th International High-Level Radioactive Waste Management Conference*, Las Vegas, Nevada, April 30–May 4, American Nuclear Society (2006).
2. P. K. SHUKLA, R. PABALAN, T. AHN, L. YANG, X. HE, and H. JUNG, "Cathodic Capacity of Alloy 22 in the Potential Yucca Mountain Repository Environment," *CORROSION/2008 Conference, paper 08583*, New Orleans, Louisiana, March 2008, NACE (2008).
3. D. S. DUNN, L. YANG, Y-M. PAN, and G. A. CRAGNOLINO, "Localized Corrosion Susceptibility of Alloy 22," *CORROSION / 2003 Conference, paper 03697*, San Diego, California, March 2003, NACE (2003).
4. D. S. DUNN, O. PENSADO, Y.-M. PAN, R. T. PABALAN, L. YANG, X. HE, and K. T. CHIANG, "Passive and Localized Corrosion of Alloy 22—Modeling and Experiments," CNWRA 2005-02, Rev. 1, San Antonio, Texas: Center for Nuclear Waste Regulatory Analyses (2005).
5. F. HUA, J. SARVER, J. JEVEC, and G. GORDON, "Corrosion Behavior of Alloy 22 and Ti Grade 7 in a Nuclear Waste Repository Environment," *Corrosion*, **60**(8), p. 764 (2004).
6. G. S. FRANKEL, "Pitting Corrosion of Metals, A Review of the Critical Factors," *Journal of the Electrochemical Society*, **145**(6), p. 2186 (1998).
7. B. KURSTEN, E. SMAILOS, I. AZKARATE, L. WERME, N. R. SMART, and G. SANTARINI, "State-of-the-Art Document on the Corrosion Behaviour of Container Materials," 5th EURATOM FRAMEWORK PROGRAMME 1998–2002 KEY ACTION: NUCLEAR FISSION, European Commission, (2004).
8. OLI SYSTEMS, INC., "A Guide to Using the OLI Software for Version 2.0 of the Analyzers," Morris Plains, New Jersey: OLI Systems, Inc. (2005).
9. M. S. GRUSZKIEWICZ, D. A. PALMER, R. D. SPRINGER, P. WANG, and A. ANDERKO, "Phase Behavior of Aqueous Na-K-Mg-Ca-Cl-NO₃ Mixtures: Isopiestic Measurements and Thermodynamic Modeling," *Journal of Solution Chemistry*, **36**, p. 723 (2007).